Decay studies for states in ^{9}Be up to 11 MeV: Insights into the $n + ^8$Be and $\alpha + ^5$He cluster structure

T. A. D. Brown,[*] P. Papka,[†] B. R. Fulton, D. L. Watson, S. P. Fox, and D. Groombridge

Department of Physics, University of York, York YO10 5DD, United Kingdom

M. Freer, N. M. Clarke, N. I. Ashwood, N. Curtis, V. Ziman, P. McEwan, and S. Ahmed

School of Physics and Astronomy, University of Birmingham, Birmingham B15 2TT, United Kingdom

W. N. Catford, D. Mahboub, C. N. Timis, and T. D. Baldwin

School of Electronics and Physical Sciences, University of Surrey, Guildford GU2 7XH, United Kingdom

D. C. Weisser

Department of Nuclear Physics, Australian National University, Canberra, ACT 0200, Australia

An experiment was performed to study the ^{9}Be(^{6}Li,^{6}Li)^{9}Be$^* \rightarrow \alpha + \alpha + n$ reaction. This experiment was designed to study the breakup of ^{9}Be in an attempt to quantify the breakup yield for each of the decay channels ($n + ^8$Be$^{g.s}$, $n + ^8$Be^{2+}, and $\alpha + ^5$He$^{g.s}$) from the low-lying states. The results suggest that the population of states in ^{9}Be from 1.68 to 11.28 MeV can be identified. Branching ratios for each of the breakup channels have been estimated for these states. These results are compared with earlier experiments and with theoretical predictions. They confirm the theoretical claim that the $n + ^8$Be^{2+} and $\alpha + ^5$He$^{g.s}$ channels increase in importance at higher excitation energies.

PACS number(s): 25.60.Gc, 26.50.+x, 21.60.Gx

I. INTRODUCTION

Due to the Borromean structure of ^{9}Be the breakup of this nucleus can, in principle, occur directly to two α particles and a neutron or via one of two unstable intermediate nuclei: ^{8}Be and ^{5}He. These two nuclei have lifetimes of 10^{-16} and 10^{-21} s, respectively, and have broad resonance states such as the first excited state in ^{8}Be at 3.04 MeV ($\Gamma \simeq 1.5$ MeV) and the ^{5}He$^{g.s.}$ ($\Gamma \simeq 0.6$ MeV).

Figure 1 illustrates the states in ^{9}Be up to $E_x = 11$ MeV as derived from proton-scattering measurements made by Dixit *et al*. [1]. Previous measurements of the breakup of ^{9}Be have mostly been concerned with breakup via those states below $E_x = 12$ MeV [2–8]. Given the available excitation energy, four channels can be identified as the principal breakup paths:

$$^9\text{Be}^* \rightarrow {}^8\text{Be}^{g.s} + n \rightarrow \alpha + \alpha + n \qquad (1)$$

$$^9\text{Be}^* \rightarrow {}^8\text{Be}^{2+} + n \rightarrow \alpha + \alpha + n \qquad (2)$$

$$^9\text{Be}^* \rightarrow {}^5\text{He}^{g.s.} + \alpha \rightarrow \alpha + n + \alpha \qquad (3)$$

$$^9\text{Be}^* \rightarrow \alpha + \alpha + n. \qquad (4)$$

The breakup of ^{9}Be via the ^{8}Be$^{g.s}$ has been quantified for many of the low-lying excited states in ^{9}Be [4,5]. However, the amount of the breakup yield going via the ^{8}Be^{2+} state and the ^{5}He$^{g.s.}$ remains uncertain. There is experimental evidence that suggests that a considerable amount of yield will go via

one of these two breakup channels for the states just above breakup threshold (those below $E_x = 4.0$ MeV), although it has not been possible to distinguish between the kinematics of these two channels [8–10]. There has also been evidence of breakup via the ^{5}He$^{g.s.}$ for the higher states in ^{9}Be although little quantitative information has been provided [9,11,12]. The contribution of the direct breakup channel has largely been ignored. However, due to the large width of the first excited state in ^{8}Be ($\Gamma \simeq 1.5$ MeV), breakup via the ^{8}Be^{2+} state has been considered a variant of direct breakup in the past [2].

The breakup of a nucleus into particular channels is correlated with the strength of the cluster configurations in the wave function for each state. There have been many theoretical models used to describe clustering in the ^{9}Be nucleus, including AMD models, which illustrate a cluster substructure in the model wave functions [13]. Recent fully microscopic cluster model calculations have also been carried out assuming $n + ^8$Be$^{g.s}$, $n + ^8$Be^{2+}, and $\alpha + ^5$He configurations [14,15]. These suggest that the latter components become dominant for higher excitation energies. However, it should be noted that the observed branching ratios for the different reaction channels will generally be governed by the presence of Coulomb and centrifugal barriers. Neither of these considerations favor breakup via $\alpha + ^5$He for those states in ^{9}Be just above breakup threshold.

The inverse of ^{9}Be breakup, the three-body formation ($\alpha\alpha n$) of ^{9}Be, may have significant astrophysical repercussions. The reaction is believed to be one of the key reactions that bridges the mass number gap at $A = 5$ and $A = 8$ in the neutron and α-particle-rich environment produced by a core collapse supernova explosion [16,17]. Previous calculations of the rate

---
[*]Present address: CENPA, Box 354290, University of Washington, Seattle, WA 98195, U.S.A.

[†]Present address: iThemba LABS, P.O. Box 722, Somerset West 7129 , South Africa.
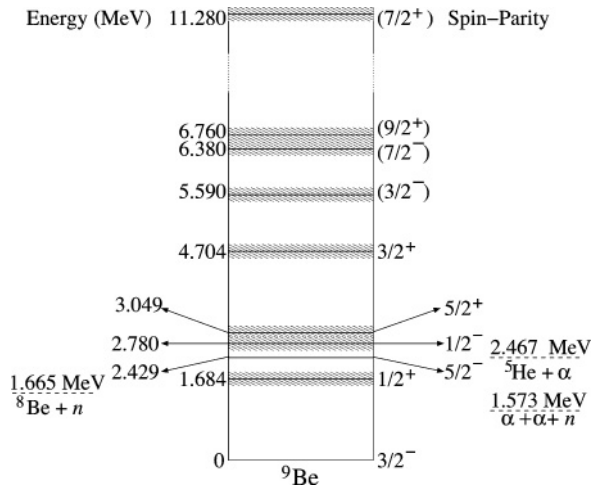
FIG. 1. The low-lying excited states in ^{9}Be derived from proton-scattering measurements made by Dixit *et al.* [1]. The states at 2.429 and 6.380 MeV are part of the ground-state rotational band.

of this reaction, including the most recent [7,18], have assumed the $\alpha\alpha n$ reaction proceeds entirely through the ^{8}Be$^{g.s.}$ for the astrophysically relevant states in ^{9}Be below 4 MeV. The short lifetimes of the ^{8}Be^{2+} state and the ^{5}He$^{g.s.}$ suggest that the sequential capture of a neutron or an α particle is very unlikely. The formalism used to derive the $\alpha\alpha n$ rate by Grigorenko and Zhukov [19] also suggests that any broad intermediate resonances will have little effect on the $\alpha\alpha n$ rate. However, another recent theoretical calculation of the $\alpha\alpha n$ rate has suggested that at temperatures above 3×10^9 K the ^{5}He$^{g.s.}$ channel becomes significant for the formation of ^{9}Be [20]. This result, along with the qualitative breakup data discussed above, suggests the necessity of acquiring quantitative branching ratio data for the low-lying states in ^{9}Be.

This article presents the results of an experiment designed to study the breakup of ^{9}Be and provide a quantitative description of the channel branching ratios for the low-lying states.

II. EXPERIMENTAL DETAILS

The experiment was performed using the 14UD pelletron tandem accelerator at the Australian National University during April 2003. The experiment was designed to study the inelastic scattering of ^{6}Li nuclei from a ^{9}Be target and the subsequent breakup of the excited ^{9}Be nuclei. The detection technique for this experiment required that the ^{6}Li recoils were detected and identified. By also detecting and identifying the two corresponding α particles for each breakup event, it is possible to reconstruct the missing momentum of the undetected neutron. The reaction kinematics are then fully defined, allowing the complete reconstruction of the breakup events and identification of the states in ^{9}Be that were populated.

A ^{6}Li beam at $E_{\text{lab}} = 60$ MeV was focused onto a ^{9}Be target (256 μg/cm^2). Data were taken for approximately 92 h with a beam current of between $I_{\text{beam}} = 2$ and 5 enA. For the purposes of detecting the α particles arising from breakup, four position-sensitive silicon strip detectors (PSSSDs) were
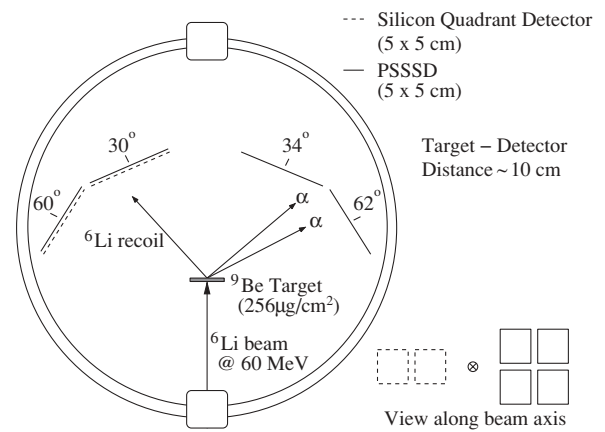

FIG. 2. Experimental setup.

used. Each detector has a thickness of $l \simeq 500$ μm and is composed of sixteen 50-mm-long resistive strips 3 mm wide. The PSSSDs typically have an energy resolution of $\delta E \simeq$ 0.2 MeV and a position uncertainty of $\Delta x \simeq \pm 0.5$ mm along a strip. As shown in Fig. 2, a pair of detector telescopes were used to detect and identify recoil ^{6}Li nuclei. Each consisted of of a silicon quadrant detector ($l \simeq 65 \mu$m) mounted in front of a PSSSD. The position of the detectors relative to the target are indicated in Fig. 2 and were chosen based on efficiency results obtained from Monte Carlo simulations.

III. ANALYSIS AND RESULTS

A. SIMSORT

For the purposes of gaining a better interpretation of the experimental results, a Monte Carlo program, SIMSORT [21], was written to simulate the breakup reaction and the detector response. SIMSORT permits the user to define the exact nature of the breakup: the excited state populated in ^{9}Be and whether breakup occurs via the ^{8}Be$^{g.s}$, the ^{8}Be^{2+} state, or the ^{5}He$^{g.s.}$. The code contains the details of the different excited states in ^{9}Be up to $E_x = 11.28$ MeV. An anisotropic distribution, determined from the spin of the initial and final states, is used for each of the breakup stages [22]. The scattering distribution used for the ^{6}Li recoils was derived from the experimental results (θ was reconstructed using the strip position information from the PSSSDs in the two telescopes). In addition to the physics governing the breakup, the energy loss and straggling in the target is also included along with details of the detector setup, i.e., threshold detection energies, the expected energy and position resolution for the PSSSDs, et cetera. For the sake of consistency with the analysis of the real data, SIMSORT uses an identical data sort process.

B. ^{8}Be$^{g.s}$ events

Figure 3 illustrates an E-ΔE spectrum plotted from data taken from both detector telescopes. Three principle loci can be easily identified on the spectrum: one corresponding to scattered ^{9}Be, another corresponding to scattered ^{6}Li, and a

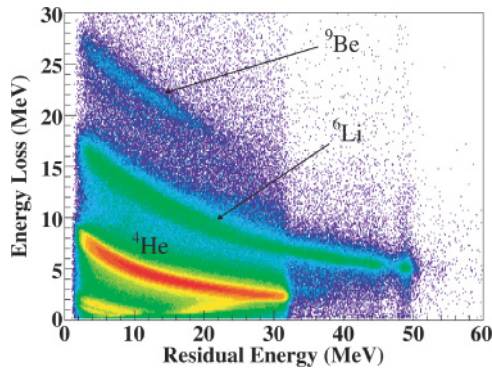FIG. 3. (Color online) E-ΔE spectrum reconstructed from data taken from both telescopes.

third arising from α particles. There is also evidence of loci corresponding to protons and deuterons at low energy.

The spectrum in Fig. 4 shows the relative energy for two particles detected in coincidence with the ^{6}Li nuclei identified in Fig. 3. The relative energy has been reconstructed assuming the two detected particles were α particles and by imposing a total energy gate consistent with ^{9}Be breakup. Events where two particles hit adjacent strips were rejected, because it is possible for a particle hitting the narrow gap between two strips to induce charge on both strips.

Three principle features can be identified from the spectrum in Fig. 4. A peak with an $E_{rel} \simeq 0.092$ MeV (Q value of ^{8}Be breakup) can be observed, corresponding to events that break up via the ^{8}Be$^{g.s.}$. A broad peak at $E_{rel} \simeq 2.8$ MeV can also be identified. This corresponds to the energy of the first excited state (2^+) in ^{8}Be and identifies events that breakup via this state. However, the large relative energy between the two α particles suggests that the events could also correspond to breakup via ^{5}He. The third feature in the spectrum, the peak lying at $E_{rel} \simeq 0.6$ MeV, does not correspond to an energy state in ^{8}Be. In the past, events in this peak have been attributed to either breakup via the tail of the broad 2^+ state in ^{8}Be ($\Gamma \simeq 1.5$ MeV) or breakup via the ^{5}He$^{g.s.}$ [8,10]. Ashwood *et al.* [10] were able to reproduce this feature using a decay phase-space calculation for both breakup via the ^{8}Be^{2+} state and breakup via the ^{5}He$^{g.s.}$.
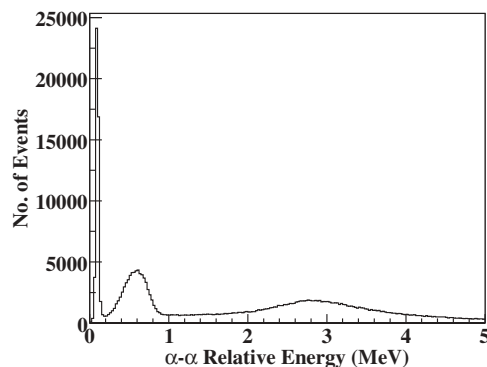

FIG. 4. α-α relative energy spectrum for events with 57 MeV $< E_{TOT} <$ 60 MeV.
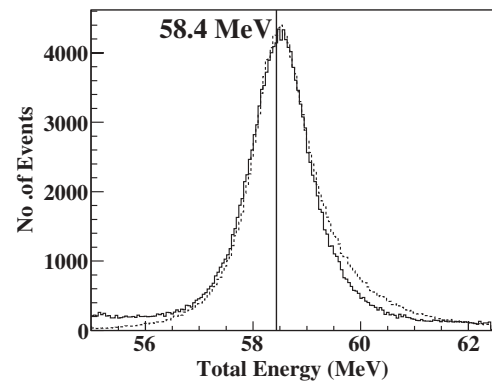

FIG. 5. Total energy spectrum for real ^{8}Be$^{g.s.}$ events (solid line) and simulated ^{8}Be$^{g.s.}$ events (dashed line).

The total final state kinetic energy (total energy) of the reaction was calculated from

$$E_{TOT} = E_{\alpha_1} + E_{\alpha_2} + E_n + E_{^6Li}, \qquad (5)$$

where the energy and momentum of the undetected neutron are reconstructed from the detected ^{6}Li and the two α particles. Figure 5 illustrates a total energy spectrum reconstructed for real ^{8}Be$^{g.s.}$ events and a simulated spectrum generated from SIMSORT. Both spectra have been corrected for energy loss in the target $E_{loss} \sim 0.1$ MeV. Given the beam energy ($E_{lab} = 60$ MeV) and the Q value of the breakup of ^{9}Be ($Q = -1.57$ MeV), the total energy of genuine ^{9}Be breakup events should be reconstructed around $E_{TOT} \simeq 58.4$ MeV. This is demonstrated in Fig. 5. The α particles detected at low energy and large angles, arising from the energy loss and straggling in the target, make the dominant contribution toward the experimental resolution.

Figure 6 shows a ^{9}Be excitation energy spectrum reconstructed for the ^{8}Be$^{g.s.}$ events identified in Fig. 4. A best fit of the state line shapes to the spectrum suggests strong contributions from the states at $E_x = 2.43$, 3.05, and 4.70 MeV. The broad state ($\Gamma \simeq 1.0$ MeV) at 2.78 MeV does not make significant contribution to the fit. A fitting routine was used such that the peak centroids were fixed
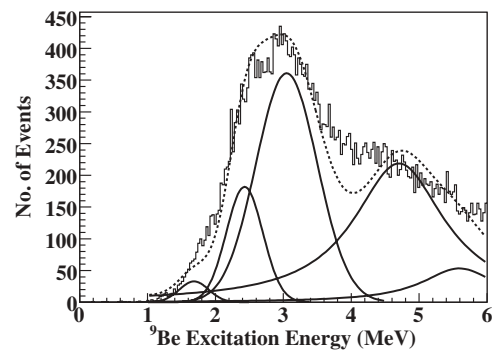

FIG. 6. ^{9}Be excitation energy spectrum for ^{8}Be$^{g.s.}$ events with 57 MeV $< E_{TOT} <$ 60 MeV. Gaussian line shapes have been used to fit the spectrum for the states at $E_x = 1.68$, 2.43, and 3.05 MeV. Due to their large intrinsic width, Lorentzian line shapes were used for the states at $E_x = 4.70$ and 5.59 MeV.

by the energy of the known states between $E_x = 1$ and 6 MeV, and the peak widths were constrained by the state intrinsic widths and the experimental resolution (obtained from Fig. 9). To remove the effect on the experimental resolution from low-energy α particles, the excitation energy was derived from the detected ^{6}Li recoil energy and angle. However, the broad width ($\Gamma = 0.632$ MeV) assigned to the narrow state at $E_x = 2.43$ MeV indicates that the experimental resolution is still poor. The dominant factors in this case are ^{6}Li energy loss and straggling in the target and the silicon quadrant detectors.

The experimental spectrum in Fig. 5 suggests that there may also be a background component to the ^{9}Be excitation energy spectrum. By gating on E_{TOT} values away from the peak region, it can be shown that such a component is approximately flat and small relative to the number of events in Fig. 6. If a linear background component is introduced into the fitting routine it has little effect on the position and width of the peaks.

The discrepancies between the fitted profile and the measured spectrum arise from the fact that, although the proton-scattering measurements of Dixit *et al.* [1] simply probe the excitation of the states, the data in this measurment reflect both the state population and the subsequent selection of one of the possible decay modes. Because the Coulomb and centrifugal barriers differ for each decay channel and, moreover, are energy dependent, imposing a decay channel selection will affect the shape as well as the apparent position of the peak resulting from a given state.

C. Neutron transfer events

Events corresponding to the neutron transfer reaction

$$^9\text{Be}(^6\text{Li}, ^7\text{Li}^*)^8\text{Be}^* \longrightarrow {}^6\text{Li} + 2\alpha + n \tag{6}$$
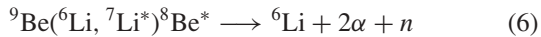
were rejected in the data sort process. This reaction has an identical Q value to ^{9}Be breakup and it was thought that it may be contaminating the breakup events of interest. The neutron transfer events were identified by reconstructing the excitation energy of the parent ^{7}Li nucleus. This is plotted in Fig. 7, and shows there is strong population of the fourth excited state in ^{7}Li ($5/2^-$) at 7.5 MeV, the first state above the neutron emission threshold at 7.2 MeV. The events that fall into this peak have been rejected when reconstructing ^{9}Be events. However, these contaminating events constitute only approximately 10% of the data and have little effect on the shape and the features of the spectra.

D. Breakup events with a large α-α relative energy

Figure 8 shows the ^{9}Be excitation energy spectrum for events identified in Fig. 4 with an α-$\alpha\, E_{rel} > 0.2$ MeV. This spectrum illustrates the population of states possibly as high as $E_x = 11$ MeV, although it is difficult to resolve individual states. As before, by deconvoluting the narrow peak just above $E_x = 2$ MeV and the broad peak centered at $E_x \simeq 6.5$ MeV, it is possible to identify the contributing states.

Figure 9 shows the ^{9}Be excitation energy spectrum for events residing in (a) the peak with α-$\alpha\, E_{rel} \simeq 0.6$ MeV and (b)
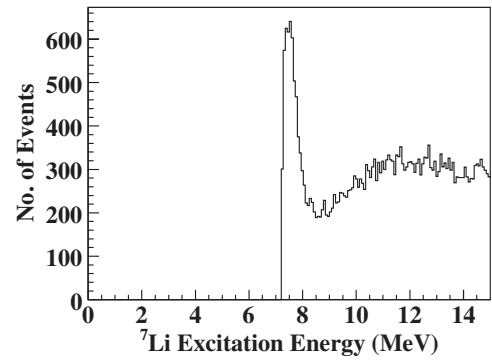

FIG. 7. ^{7}Li excitation energy specrum for ^{8}Be$^{g.s.}$ events with 57 MeV $< E_{TOT} < 60$ MeV.

the peak with α-$\alpha\, E_{rel} \simeq 2.8$ MeV. It can be seen from Fig. 9(a) that these events break up mostly via the state at $E_x = 2.43$ MeV. The line shapes fitted to the spectrum indicate there is also a contribution from the state at $E_x = 3.05$ MeV. The widths for the line shapes obtained in this fit were used to fix the width of the line shapes used in Fig. 6. The spectrum in Fig. 9(b) indicates that these events populate only those states in ^{9}Be above $E_x = 4.0$ MeV. Strong contributions can be seen from the states at $E_x = 6.38$ and 6.76 MeV. Lorentzian line shapes have been used to fit the spectrum for all these broad ($\Gamma > 1.0$ MeV) states.

The quality of the fit to the spectrum in Fig. 9(b) is again affected by the distortion of the states associated with feeding to the ^{8}Be^{2+} state/^{5}He$^{g.s.}$, but also possibly by the presence of other states in the 4- to 12-MeV region [23].

The issue of whether these events break up via the ^{5}He$^{g.s.}$ or the ^{8}Be^{2+} state was resolved by analyzing the α-n relative energy. The detected breakup α particles were randomly labeled α_1 and α_2 in the data sort process. Figure 10 illustrates a series of spectra where the α_1-n relative energy has been plotted against the α_2-n relative energy. These spectra have been reconstructed for regions of excitation energy corresponding to the known states in ^{9}Be between $E_x = 2.43$ and 11.28 MeV. The Q value for ^{5}He breakup is $Q \simeq 0.9$ MeV ($\Gamma \simeq 0.65$ MeV), and therefore the presence of ^{5}He$^{g.s.}$ events in the spectra should be indicated by event concentrations around $E_{rel} = 0.9$ MeV on one axis and around a relatively

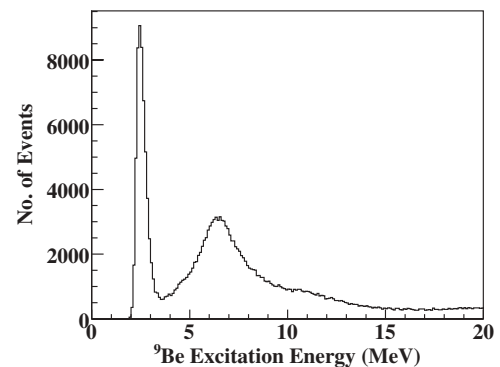FIG. 8. ^{9}Be excitation energy spectrum for ^{9}Be breakup events with α-$\alpha\, E_{rel} > 0.2$ MeV.

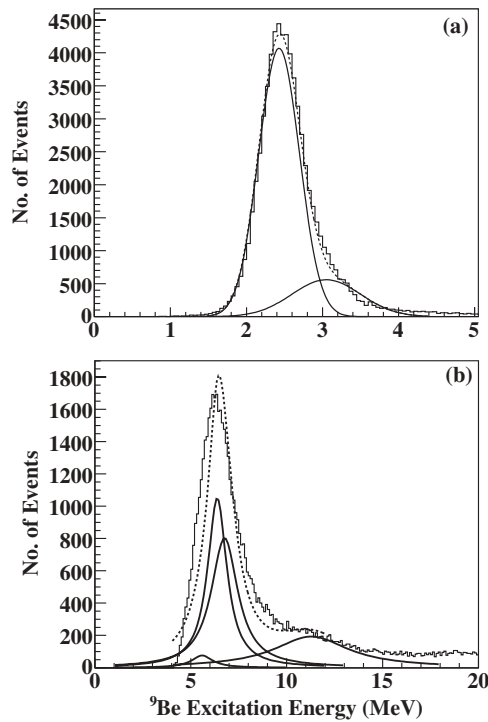FIG. 9. ^{9}Be excitation energy spectrum for (a) break-up events with 0.2 MeV $< \alpha$-$\alpha E_{rel} < 1.0$ MeV and (b) breakup events with 2.5 MeV $< \alpha$-$\alpha E_{rel} < 3.5$ MeV. Gaussian line shapes were used for the fit in (a) and Lorentzian line shapes were used for the fit in (b).

higher energy on the other axis. The α particle originating from the ^{5}He should have a smaller relative energy with the neutron than the other α particle (originating from the first stage of the breakup), assuming there is enough available energy for the first emitted α particle.

Event concentrations in Fig. 10 around 0.9 MeV suggest that there is evidence for breakup via ^{5}He for states at $E_x = 6.38$ and 6.76 MeV, although it is not clear whether such features can be identified from the other spectra. By using 1D projections of the α-n relative energy spectra it is possible to distinguish events associated with breakup via the ^{8}Be^{2+} and ^{5}He$^{g.s.}$ for all those states above $E_x = 4.0$ MeV.

E. Breakup path for states in ^{9}Be above 4.0 MeV

A plot of the α_1-n relative energy for an energy region consistent with the 6.38-MeV state is given in Fig. 11. Two spectrum profiles are shown corresponding to genuine and simulated events. ^{8}Be$^{g.s.}$ events have not been included in either of the spectra, and events with α_2-$n E_{rel} < 2.0$ MeV have also been rejected for the purposes of enhancing features associated with ^{8}Be^{2+} and ^{5}He$^{g.s.}$ events.

The simulated spectrum was generated for events assuming a ^{5}He$^{g.s.}$ breakup path. This spectrum is a good match to the experimental profile, suggesting that most of the events in this excitation energy region breakup via the ^{5}He$^{g.s.}$. Figure 12 shows a simulated spectrum for events assuming a ^{8}Be^{2+} breakup path.
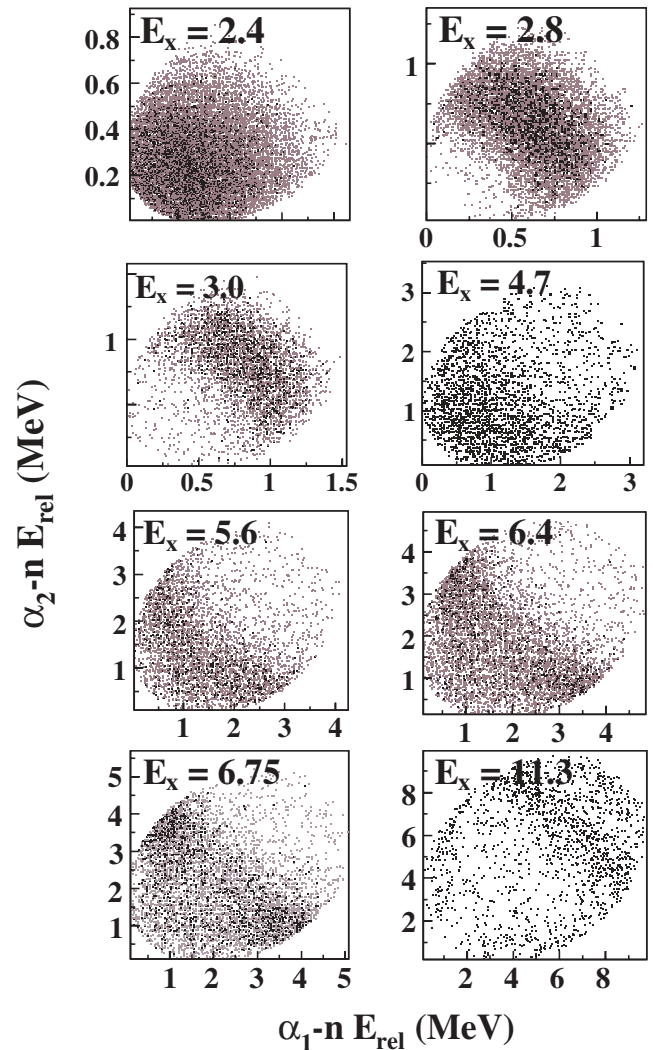

FIG. 10. (Color online) 2D α-n relative energy spectra for ^{9}Be excitation energies above 2.3 MeV. Events have been selected for each spectrum by gating on an excitation energy region of 0.2 MeV centered on the value given in each plot. ^{8}Be$^{g.s.}$ events have been removed.

For the states at high energy it is possible to reproduce the α-n relative energy spectra by simulating events for either one type of breakup path or the other, or by mixing the two types of events and weighting each channel appropriately. The proportion of breakup yield associated for each breakup path can now be determined. The number of events going via the ^{8}Be$^{g.s.}$ can be easily obtained from an α-α relative energy spectrum.

F. Breakup path for the 2.43-MeV state

The identification of the breakup path for states in ^{9}Be with an $E_x < 4.0$ MeV, i.e., those states that are more likely to be important in an astrophysical environment, is more difficult. Although it is trivial to identify ^{8}Be$^{g.s.}$ events, at low excitation energy the α-n relative energy for ^{5}He$^{g.s.}$ and ^{8}Be^{2+} events is very difficult to distinguish. This problem is especially acute

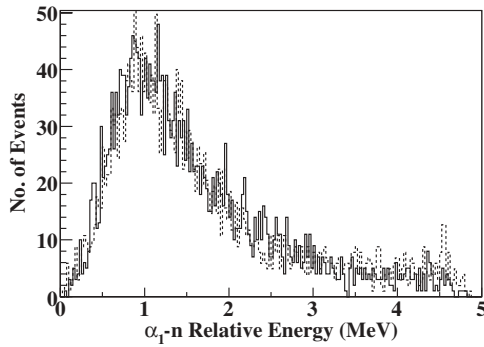FIG. 11. α_1-n relative energy spectrum for simulated (dashed line) and real (solid line) data events. The simulated events have been generated assuming breakup via the $^5\mathrm{He}^{\mathrm{g.s.}}$. Both spectra have been reconstructed for 6.3 MeV $<$ $^9\mathrm{Be}$ E_x $<$ 6.5 MeV and α_2-n E_{rel} $>$ 2.0 MeV.

for the excitation energy region around the state at E_x = 2.43 MeV.

Previous attempts to distinguish between these channels have not been successful [3,8,10]. Recently we have shown that by looking instead at the angular correlation, a separation is possible [22]. This work confirmed the small (6%) branching ratio to the $n + {}^8\mathrm{Be}^{\mathrm{g.s.}}$ channel and showed that the remaining decay was primarily to the $^8\mathrm{Be}^{2+}$ channel.

G. Breakup path for the other states below E_x = 4.0 MeV

For the energy region around the states at E_x = 2.78 and 3.05 MeV, there are very few breakup events associated with either of these states. The poor statistics means that it is very difficult to use any of the previous methods to distinguish the $^8\mathrm{Be}^{2+}$ and $^5\mathrm{He}^{\mathrm{g.s.}}$ breakup channels. Figure 13 illustrates the α-α relative energy spectrum for breakup events with an excitation energy consistent with the 3.05-MeV state. To avoid being overwhelmed with events from the state at E_x = 2.43 MeV, an additional gate has been imposed excluding $^6\mathrm{Li}$ events consistent with a kinematic locus defined by the 2.43-MeV state.
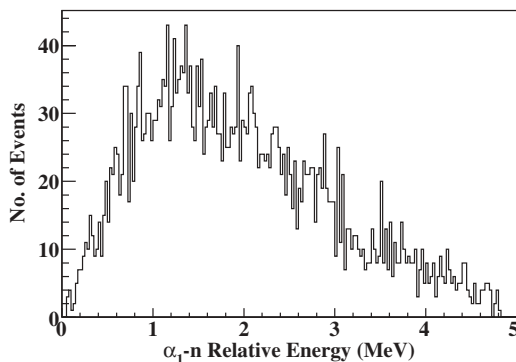

FIG. 12. Simulated α_1-n relative energy spectrum for $^8\mathrm{Be}^{2+}$ events with 6.3 MeV $<$ $^9\mathrm{Be}$ E_x $<$ 6.5 MeV and α_2-$n E_{\mathrm{rel}}$ $>$ 2.0 MeV.

The small number of events that lie above $E_{\mathrm{rel}} = 0.2$ MeV in Fig. 13 are suspected to be events associated with the $^8\mathrm{Be}^{2+}$ and/or $^5\mathrm{He}^{\mathrm{g.s.}}$ breakup channels. Using this data it is possible to establish an upper limit on the breakup yield for the $^8\mathrm{Be}^{2+}$ and $^5\mathrm{He}^{\mathrm{g.s.}}$ channels.

H. Results

Table I lists the estimated branching ratio and corresponding detection efficiency for states in $^9\mathrm{Be}$ up to E_x = 11.28 MeV. For the states above E_x = 2.43 MeV, the events have been selected by gating on energy regions of 0.2 MeV approximately centered on each state. To overcome the problem of poor statistics around the state at E_x = 11.28 MeV, an energy window of 0.4 MeV was used for this case. A branching ratio value has not been estimated for the state at 5.59 MeV. This state's event contribution is very small, and the number of events in the energy region around this state are dominated by the adjacent states. Given the large amount of overlap between the states at E_x = 6.38 and 6.76 MeV, a combined branching ratio has been quoted for both of these states.

The detection efficiencies have been determined using SIMSORT for the angular range covered by the detectors. The absolute efficiency values given in Table I were determined using isotropic center-of-mass breakup distributions. Although these values are different if an anisotropy is used, their value relative to one another for a given breakup path (which ultimately determines the branching ratio) is relatively insensitive to this change.

TABLE I.

$^9\mathrm{Be}$ state/ΔE_x	BC[a]	$\epsilon(\%)$[b]	BR (%)[c]
1.684 MeV	$^8\mathrm{Be}^{\mathrm{g.s.}}$	0.5	100
	$^8\mathrm{Be}^{2+}$	2.8	0
2.429 MeV	$^8\mathrm{Be}^{\mathrm{g.s.}}$	3.5	6 ± 1
	$^8\mathrm{Be}^{2+}$	2.5	94 ± 2
	$^5\mathrm{He}^{\mathrm{g.s.}}$	2.7	<5
2.780 MeV[d]	$^8\mathrm{Be}^{\mathrm{g.s.}}$	3.4	32 ± 15
(2.7–2.9)	$^8\mathrm{Be}^{2+}$	2.5	< 69
	$^5\mathrm{He}^{\mathrm{g.s.}}$	2.7	< 67
3.049 MeV[d]	$^8\mathrm{Be}^{\mathrm{g.s.}}$	3.4	46 ± 20
(2.95–3.15)	$^8\mathrm{Be}^{2+}$	2.5	< 55
	$^5\mathrm{He}^{\mathrm{g.s.}}$	2.6	< 54
4.704 MeV	$^8\mathrm{Be}^{\mathrm{g.s.}}$	3.3	16 ± 2
(4.6–4.8)	$^8\mathrm{Be}^{2+}$	1.8	43 ± 20
	$^5\mathrm{He}^{\mathrm{g.s.}}$	1.9	41 ± 20
6.380 / 6.760 MeV	$^8\mathrm{Be}^{\mathrm{g.s.}}$	3.2	4 ± 1
(6.3–6.85)	$^8\mathrm{Be}^{2+}$	1.5	7 ± 3
	$^5\mathrm{He}^{\mathrm{g.s.}}$	1.1	89 ± 35
11.280 MeV	$^8\mathrm{Be}^{\mathrm{g.s.}}$	3.2	3 ± 1
(11.1–11.5)	$^8\mathrm{Be}^{2+}$	1.1	21 ± 8
	$^5\mathrm{He}^{\mathrm{g.s.}}$	0.2	76 ± 30

[a]Breakup channel.
[b]Detection efficiency.
[c]Branching ratio corrected for detection efficiency.
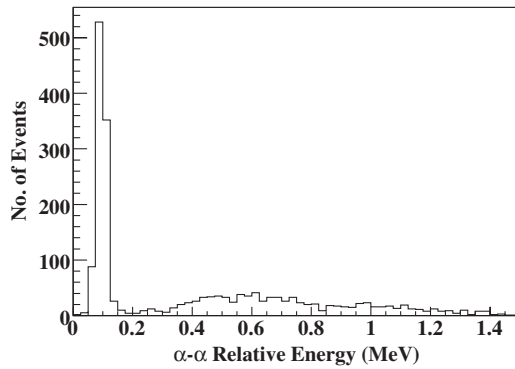[d]Most events associated with the 2.43-MeV state have been removed.

FIG. 13. α-α relative energy spectrum for ^{9}Be breakup events with $2.95 < {}^9$Be $E_x < 3.15$ MeV. Most events associated with the 2.43-MeV state have been removed.

Errors have been estimated for each branching ratio, and are primarily based on the effect of overlapping adjacent states and our ability to distinguish the kinematic features associated with the different channels.

IV. DISCUSSION AND CONCLUSIONS

Genuine ^{9}Be breakup events have been identified and excitation energy spectra have been reconstructed illustrating the population of low-lying states in ^{9}Be. The branching ratio of each breakup path has been estimated for states in ^{9}Be up to $E_x = 11.28$ MeV.

The branching ratios calculated for $E_x > 4.0$ MeV have confirmed that the ^{5}He$^{g.s.}$ breakup channel plays a significant role as we move to higher energy and confirms the observations of breakup via ^{5}He$^{g.s.}$ made by Prezado [9], Soić [12], and Nyman [11]. The values given for feeding to the ^{8}Be$^{g.s.}$ are broadly consistent with the values determined by Cocke and Christensen [5]. The large ^{5}He$^{g.s.}$ branching ratio for the energy region corresponding to the states at $E_x = 6.38$ and 6.76 MeV is due to the 6.38-MeV membership of the ground-state (g.s.) rotational band. The ^{9}Be$_{g.s.}$ is predicted to have a ^{5}He $+\alpha$ structure [14].

The branching ratio results obtained from the 2.43-MeV state are discussed in Ref. [22]. For the other two states just above breakup threshold ($E_x = 2.78$ and 3.05 MeV), it has been shown that between 30 and 50% of events populating these states decay to ^{8}Be$^{g.s.}$, leaving the remaining events to decay either via the ^{8}Be^{2+} state or via the ^{5}He$^{g.s.}$. Unfortunately, there were not enough data to identify the relative contributions for these two breakup channels. The branching ratio estimate for the 3.05-MeV state to the ^{8}Be$^{g.s.}$ seems small compared to the value given by Christensen and Cocke ($87 \pm 13\%$), although not unreasonable. The method used to remove contaminating events from the state at $E_x = 2.43$ MeV was only partially successful. The large uncertainty given for the ^{8}Be$^{g.s.}$ branching ratio reflects this outcome. The branching ratio estimate for the 2.78-MeV state to ^{8}Be^{2+}/^{5}He$^{g.s.}$ is consistent with Prezado's remark [9] that a considerable contribution of the breakup does not go via the ^{8}Be$^{g.s.}$ for this state.

The present results compare favorably with theoretical predictions as well as other experimental results. Descouvemont [15] calculated reduced widths for the three different channels using a microscopic three-cluster model of ^{9}Be for states with a spin of up to 9/2. The reduced width and the branching ratio for a given channel are related by an unknown penetrability, the calculation of which is not trivial for broad intermediate states such as the ^{8}Be^{2+} state and the ^{5}He$^{g.s.}$. However, it can be shown that the branching ratios do reproduce the theoretical trend of these reduced widths.

The astrophysical implications of these new branching ratios are unclear. For the astrophysically relevant states, with the exception of the 2.43-MeV state, this work provides only upper limits for the ^{5}He$^{g.s}$ and the ^{8}Be^{2+} channels. Although it is clear that a significant portion of the breakup yield for these states does not go via the ^{8}Be$^{g.s.}$, this may have little effect on the $\alpha\alpha n$ rate. Buchmann *et al.* [20] derived the population density for the three intermediate states over a temperature range applicable to the site for the $\alpha\alpha n$ reaction in a supernova. The results indicate that the ^{8}Be^{2+} state will not contribute significantly to the $\alpha\alpha n$ rate.

[1] S. Dixit *et al.*, Phys. Rev. C **43**, 1758 (1991).

[2] D. Bodansky, S. F. Eccles, and I. Halpern, Phys. Rev. **108**, 1019 (1957).

[3] J. Mösner, G. Schmidt, and S. Schintlmeister, Nucl. Phys. **64**, 169 (1965).

[4] P. R. Christensen and C. L. Cocke, Nucl. Phys. **89**, 656 (1966).

[5] C. L. Cocke and P. R. Christensen, Nucl. Phys. **A111**, 623 (1968).

[6] H. Utsunomiya, Y. Yonezawa, H. Akimune, T. Yamagata, M. Ohta, M. Fujishiro, H. Toyokawa, and H. Ohgaki, Phys. Rev. C **63**, 018801 (2000).

[7] K. Sumiyoshi, S. Goko, and T. Kajino, Nucl. Phys. **A709**, 467 (2002).

[8] B. R. Fulton *et al.*, Phys. Rev. C **70**, 047602 (2004).

[9] Y. Prezado *et al.*, Phys. Lett. **B618**, 43 (2005).

[10] N. Ashwood *et al.*, Phys. Rev. C **72**, 024314 (2005).

[11] G. Nyman *et al.*, Nucl. Phys. **A510**, 189 (1990).

[12] N. Soić *et al.*, Europhys. Lett. **41**, 489 (1998).

[13] Y. Kanada-En'yo, H. Horiuchi, and A. Ono, Phys. Rev. C **52**, 628 (1995).

[14] K. Arai, P. Descouvemont, D. Baye, and W. N. Catford, Phys. Rev. C **68**, 014310 (2003).

[15] P. Descouvemont, Eur. Phys. J. A **12**, 413 (2001).

[16] S. E. Woosley and R. S. Hoffman, Astrophys. J. **395**, 202 (1992).

[17] S. E. Woosley, J. R. Wilson, G. J. Mathews, R. D. Hoffman, and B. S. Meyer, Astrophys. J. **433**, 229 (1994).

[18] C. Angulo *et al.*, Nucl. Phys. **A656**, 3 (1999).

[19] L. V. Grigorenko and M. V. Zhukov, Phys. Rev. C **72**, 015803 (2005).

[20] L. Buchmann, E. Gete, J. C. Chow, J. D. King, and D. F. Measday, Phys. Rev. C **63**, 034303 (2001).

[21] P. Papka, SIMSORT (unpublished).

[22] P. Papka *et al.*, Phys. Rev. C **75**, 045803 (2007).

[23] F. Ajzenberg-Selove, Nucl. Phys. **A490**, 1 (1988).